Molecular Crystals and Liquid Crystals Science and Technology. Section A. Molecular Crystals and Liquid Crystals

Publication details, including instructions for authors and subscription information:
http://www.tandfonline.com/loi/gmcl19

Computer Simulation of Steady Shear Flow of Liquid Crystals with the Gay-Berne Potential

N. Mori [a] , J. Morimoto [a] & K. Nakamura [a]

[a] Department of Mechanical Engineering, Osaka University, Suita, Osaka, 565, Japan

Version of record first published: 04 Oct 2006

To cite this article: N. Mori, J. Morimoto & K. Nakamura (1997): Computer Simulation of Steady Shear Flow of Liquid Crystals with the Gay-Berne Potential, Molecular Crystals and Liquid Crystals Science and Technology. Section A. Molecular Crystals and Liquid Crystals, 307:1, 1-15

To link to this article: http://dx.doi.org/10.1080/10587259708047083

Mol. Cryst. Liq. Cryst., 1997, Vol. 307, pp. 1–15
Reprints available directly from the publisher
Photocopying permitted by license only

Computer Simulation of Steady Shear Flow of Liquid Crystals with the Gay-Berne Potential

N. MORI*, J. MORIMOTO and K. NAKAMURA

Department of Mechanical Engineering, Osaka University, Suita, Osaka 565, Japan

(Received 29 December 1995; In final form 5 August 1996)

Computer simulations of steady shear flow of nematic phases are performed using a non-equilibrium molecular dynamics. The SLLOD-type algorithm is applied to the shear flows of Gay-Berne fluids which are nematic in the equilibrium states. Two Gay-Berne potentials with $\mu = 1$, $\nu = 2$ and $\mu = 2$, $\nu = 1$ are used and both molecular aspect ratios are set equal to 3. In the initial stage of shearing various patterns of the transient behavior are found in the order parameter and orientation angle, according to the initial conditions and shear rate. In the steady state the director is inclined to the flow at a constant angle regardless of the shear rate and the system becomes more highly oriented state. The fluids exhibit shear-thinning in viscosity and non-zero first and second normal stress differences.

Keywords: SLLOD algorithm; liquid crystalline molecule; Gay-Berne potential; steady shear flow; rheological properties

1. INTRODUCTION

Molecular dynamics simulations of liquid crystalline molecules at equilibrium have been carried out actively. Gay-Berne potential [1] has been used as a model potential for liquid crystalline molecules and many calculations for a phase transition have been performed [2–4]. Yoshida *et al.* [5] used a model molecule composed of a linear array of spherical interaction elements to study the nematic-isotropic phase transition using the Monte

*Corresponding author: Department of Mechanical Engineering, Faculty of Engineering, Osaka University, 2-1 Yamadaoka Suita, Osaka 565, Japan.

Carlo method. As computers become more powerful, the use of real liquid crystalline molecules like 4-*n*-pentyl-4′-cyanobiphenyl(5CB) has been attempted for reproduction of exact experimental data [6–8]. These simulations of realistic systems, however, may involve difficulties in providing a straightforward insight into the nature of intermolecular interactions responsible for the formation of liquid crystalline phase, because all possible contributions from various types of interactions can be hardly separated.

Nonequilibrium molecular dynamics (NEMD) is a technique used to simulate the behavior of a system subjected to an external field. The SLLOD algorithm was originally developed for the shear flow of atomic liquids by Evans and Morris [9]. The rheological behavior of *n*-alkanes was calculated by using the SLLOD algorithm and it was found that the shear-thinning at low shear rates and shear-thickening at high shear rates were observed in the viscosities [10–12]. Viscometric functions of polymeric fluids modeled by a finitely extensible nonlinear elastic (FENE) and generalized Lennard-Jones (GLJ) dumbbells have been investigated [13]. Recently, Dlugogorski *et al.* developed the SLLOD algorithm for the Gay-Berne potential, which is ellipsoid of revolution, by taking a fluid vorticity into account [14]. They calculated the rheology and the structure of systems composed of ellipsoids of revolution in a isotropic phase, and found the build-up of a highly ordered structure exhibiting global orientation of particle in the direction of the vorticity axis.

In the present work, we simulate the steady shear flows of liquid crystalline molecules in a nematic phases at equilibrium. We use the Gay-Berne potential and apply the SLLOD-type algorithm developed by Dlugogorski [14] to the present simulations. First, the nematic phase at the initial condition of the steady shear flows is obtained by means of the equilibrium calculations. Then, the steady shear flow is imposed upon the nematic phase using the SLLOD-type algorithm and the Lees-Edwards (LE) boundary conditions [15]. We examine the change of structure of the system including a transient behavior in the start-up flow, and the rheological properties.

2. POTENTIAL AND NEMD SIMULATION ALGORITHM

Gay and Berne proposed a function which gave the best fit to the pair potential for the molecule consisting of four Lennard-Jones atoms separated by a distance of $(2/3)\sigma$; σ is the collision radius of the Lennard-Jones atom

[1]. The so-called Gay-Berne potential is

$$\phi_{GB}(\hat{\boldsymbol{u}}_i, \hat{\boldsymbol{u}}_j, \boldsymbol{r}) = 4\varepsilon(\hat{\boldsymbol{u}}_i, \hat{\boldsymbol{u}}_j, \hat{\boldsymbol{r}})\left\{\left(\frac{\sigma_0}{r - \sigma(\hat{\boldsymbol{u}}_i, \hat{\boldsymbol{u}}_j, \hat{\boldsymbol{r}}) + \sigma_0}\right)^{12} - \left(\frac{\sigma_0}{r - \sigma(\hat{\boldsymbol{u}}_i, \hat{\boldsymbol{u}}_j, \hat{\boldsymbol{r}}) + \sigma_0}\right)^{6}\right\}, \tag{1}$$

where $\hat{\boldsymbol{u}}_i$, $\hat{\boldsymbol{u}}_j$ are the unit vector giving the orientation of the two molecules and $\hat{\boldsymbol{r}}$ is the unit vector along the intermolecular vector $\boldsymbol{r} = \boldsymbol{r}_i - \boldsymbol{r}_j$. Here, the well depth of the potential $\varepsilon(\hat{\boldsymbol{u}}_i, \hat{\boldsymbol{u}}_j, \hat{\boldsymbol{r}})$ and the intermolecular separation $\sigma(\hat{\boldsymbol{u}}_i, \hat{\boldsymbol{u}}_j, \hat{\boldsymbol{r}})$ are orientation-dependent Lennard-Jones parameters, and their full expressions contain four model parameters; ratio σ_e/σ_s, ratio $\varepsilon_e/\varepsilon_s$, μ and ν (see [1] for explicit expression). σ_e/σ_s is the molecular aspect ratio, $\varepsilon_e/\varepsilon_s$ the ratio of the well depths for the end-to-end and side-by-side configurations and μ and ν are treated as adjustable parameters.

In the present work, σ_e/σ_s is set equal to 3 and $\varepsilon_e/\varepsilon_s$ is equal to 0.5. Two sets of parameter for μ and ν are used: $(\mu, \nu) = (1, 2)$ and $(2, 1)$. The difference of these parameters does not affect the relative well depths for the side-by-side or end-to-end configurations and the side-by-side configuration is relatively more stable with respect to the cross and tee configurations for both potentials. However, the well for the side-by-side configuration of the potential with $(\mu, \nu) = (1, 2)$ is deeper and therefore the strong intermolecular force is expected. We will call the potential with $(\mu, \nu) = (1, 2)$ the strong potential and that with $(\mu, \nu) = (2, 1)$ the weak potential.

In the case of Lennard-Jones particle, the NEMD simulations for shear flows have been performed using the SLLOD algorithm, which was developed by Morris and Evans [9]. The translational equations of motion in the SLLOD algorithm are

$$\dot{\boldsymbol{r}}_i = \boldsymbol{p}_i/m_i + \boldsymbol{r}_i \cdot \nabla \boldsymbol{u} \tag{2}$$

$$\dot{\boldsymbol{p}}_i = \boldsymbol{F}_i - \boldsymbol{p}_i \cdot \nabla \boldsymbol{u} - \alpha_1 \boldsymbol{p}_i \tag{3}$$

where $\boldsymbol{r}_i$, $\boldsymbol{p}_i$ and $\boldsymbol{F}_i$ are the position, the peculiar linear momentum and the force according to the ith molecule. $\boldsymbol{u}$ represents the field of the fluid velocity. α_1 is derived by use of Gauss's principle of constraint and for a

steady simple shear flow it is given by

$$\alpha_1 = \frac{\Sigma_{i=1}^{N} \boldsymbol{p}_i \cdot \boldsymbol{F}_i - \dot{\gamma} \Sigma_{i=1}^{N} p_{ix} p_{iy}}{\Sigma_{i=1}^{N} \boldsymbol{p}_i^2}, \tag{4}$$

where $\dot{\gamma}$ is the shear rate.

For the rigid bodies such as Gay-Berne-like molecules, the rotational equations of motion are required. Dlugogoski *et al.* [14] proposed a new form of the SLLOD algorithm with extra terms due to the explicit coupling between the velocity field and the rotational motion of molecules. The SLLOD-like modification for the rotational equations of motion is given by

$$\dot{\boldsymbol{L}}_i = \boldsymbol{T}_i - \alpha_2 \boldsymbol{L}_i \tag{5}$$

$$\boldsymbol{L}_i = \boldsymbol{I}_i \boldsymbol{\omega}_i \tag{6}$$

$$\boldsymbol{\omega}_i = \hat{\boldsymbol{\omega}}_i + \boldsymbol{\Omega}, \tag{7}$$

where $\boldsymbol{L}_i$ and $\boldsymbol{T}_i$ are the angular momentum and the torque. $\boldsymbol{I}_i$ represents the inertia tensor. The angular velocity $\boldsymbol{\omega}$ is the sum of the peculiar angular velocity $\hat{\boldsymbol{\omega}}$ and the vorticity field $\boldsymbol{\Omega}$, where $\boldsymbol{\Omega} = \mathrm{rot}\boldsymbol{u}$. α_2 is given by

$$\alpha_2 = \frac{\Sigma_{i=1}^{N} \{\boldsymbol{L}_{pi} \times (\hat{\boldsymbol{\omega}}_{pi} + \boldsymbol{\Omega}_{pi}) + \boldsymbol{T}_{pi} - \boldsymbol{I}_{pi} \dot{\boldsymbol{R}}_i \boldsymbol{\Omega}\} \cdot \hat{\boldsymbol{\omega}}_{pi}}{\Sigma_{i=1}^{N} \boldsymbol{L}_{pi} \cdot \hat{\boldsymbol{\omega}}_{pi}} \tag{8}$$

for the steady shear flows. Suffix p denotes the values according to body fixed coordinates, and $\boldsymbol{R}$ is the rotation matrix. If $\dot{\gamma} = 0$, then Eqs. (2)–(8) reduce to the equations for the equilibrium states.

These equations of motion are implemented in conjunction with the periodic boundary conditions of Lees and Edwards [15]. The schematic description of the Lees-Edwards boundary conditions is shown in Figure 1. The row of bricks immediately above the central cube slides with uniform velocity $\dot{\gamma}L$ in the positive x-direction and the row of bricks below the central cube slides with $-\dot{\gamma}L$. If a molecule passes through the top face as shown in Figure 1, then the position and velocity of the molecule are replaced by

$$\boldsymbol{r}_i^{new} = (\boldsymbol{r}_i - \dot{\gamma} L t \boldsymbol{e}_x) \bmod L, \tag{9}$$

$$\dot{\boldsymbol{r}}_i^{new} = \dot{\boldsymbol{r}}_i - \dot{\gamma} L \boldsymbol{e}_x, \tag{10}$$

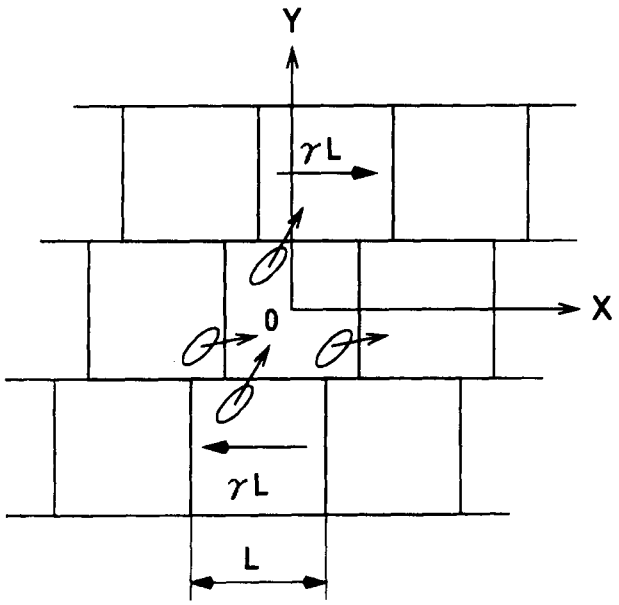

FIGURE 1 Schematic description of Lees-Edwards boundary conditions.

where t is the time and e_x the unit vector in the positive x-direction. If the molecule passes through the bottom surface, a similar procedure of replacing should be done.

Dimensionless quantities, denoted by an asterisk superscript, are used in the present simulation. For example, the dimensionless length, linear momentum, time and temperature are defined as

$$r^* = \frac{r}{\sigma_0}, \quad p^* = \frac{p}{\sqrt{m\varepsilon_0}}, \quad t^* = \frac{t}{\sqrt{m\sigma_0^2/\varepsilon_0}}, \quad T^* = \frac{k_B T}{\varepsilon_0}, \tag{11}$$

where k_B is the Boltzmann constant.

The order parameter S and the director $\boldsymbol{n}$ of the system were calculated during the simulation. The order parameter is defined as the largest eigenvalue of the Q-tensor:

$$Q_{\alpha\beta} = \frac{1}{N}\sum_{i=1}^{N}\left(\frac{3\hat{u}_{i\alpha}\hat{u}_{i\beta} - \delta_{\alpha\beta}}{2}\right). \tag{12}$$

The director is obtained as the corresponding eigenvector.

The stress tensor is given by

$$\sigma_{\alpha\beta} = -\frac{1}{V}\left\langle \sum_{i=1}^{N} \frac{p_{i\alpha} p_{i\beta}}{m_i} + \sum_{i=1}^{N-1} \sum_{j>i}^{N} r_{ij\alpha} F_{ij\beta} \right\rangle \tag{13}$$

Therefore the viscometric functions are defined as follows,

$$\eta_1 = \sigma_{xy}/\dot{\gamma}, \tag{14}$$

$$\eta_2 = \sigma_{xy}/\dot{\gamma}, \tag{15}$$

$$N_1 = \sigma_{xx} - \sigma_{yy}, \tag{16}$$

$$N_2 = \sigma_{yy} - \sigma_{zz}, \tag{17}$$

where η_1 and η_2 are the shear viscosities, N_1 and N_2 are the first and second normal stress differences, and V denotes the total volume of the primitive cube.

The equations of motion were solved by the modified leap-flog method using time step of between 0.001 for high and 0.002 for low shear rates. All the simulations were performed for 108 molecules in a cubic box where Lees-Edwards boundary conditions [15] were applied. As the shear was imposed upon the equilibrium states at the time $t = 0$, the structure of the system showed the transient behavior. Therefore the data of steady states were collected after the initial 100,000 time steps.

Before the shear calculations the equilibrium calculations were carried out for various temperatures. Figure 2 shows the temperature dependence of order parameter. A scaled number density $\rho^*(= N\sigma_0^3/V)$ is set equal to 0.3. The system was found to form a variety of meso-phases as the temperature was lowered. In the present work, we used the nematic phases as the initial states where the shear flows were imposed.

3. RESULTS AND DISCUSSION

3.1. Transient Behavior

Since the Heaviside shear rate function is imposed upon the system which is initially at equilibrium, the structure of the system changes largely at the initial stage of the flow. It is expected that pattern of the transient behavior

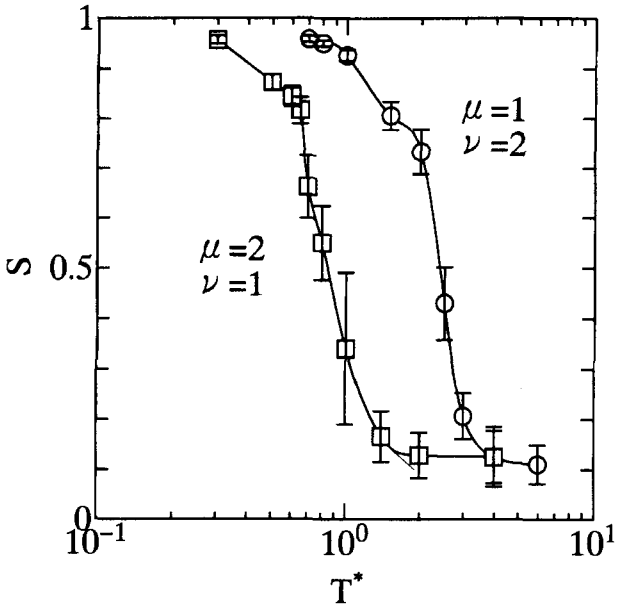

FIGURE 2 Temperature dependence of order parameter.

depends on the initial conditions of the order parameter and orientation angle, and on the magnitude of shear rate.

Figure 3(a) shows the change of the orientation angle θ_x with time, and Figure 3(b) shows the corresponding change of the order parameter. The angle θ_x in the equilibrium state cannot be controlled because of the periodic boundary condition. Therefore we examined the dependence of θ_x on the transient behavior by imposing the shear flows with opposite directions; a positive and negative shearing. In Figure 3 the shear flow is imposed upon the same initial state for the weak potential; $T^* = 0.7$, $S_0 = 0.690$, $\theta_{x0} = 7.82°$. θ_x rapidly increases and approaches the steady state with a fluctuation for $\dot{\gamma}^* = 1$. In the steady shear flow of real low molecular liquid crystals, the director is inclined at a constant angle for aligning nematic LCs and tumbles for tumbling nematic ones. However only the aligning behavior was observed in the present calculations. For the negative shear flow of $\dot{\gamma}^* = -1$, which means that the shear flow is imposed in the opposite direction, the director rapidly rotates in the opposite direction of vorticity of the flow field and is inclined to the flow direction at the same angle as for $\dot{\gamma}^* = 1$. The order parameter increases and asymptotically approaches the steady value for $\dot{\gamma}^* = 1$, while for $\dot{\gamma}^* = -1$ it significantly decreases at first

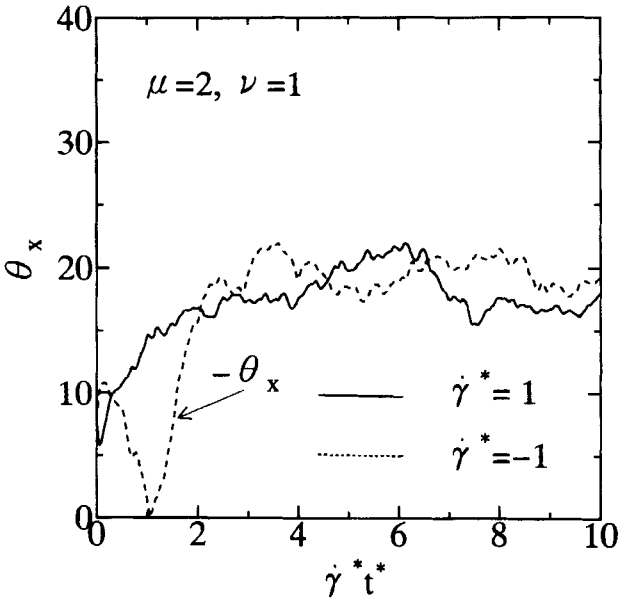

(a)

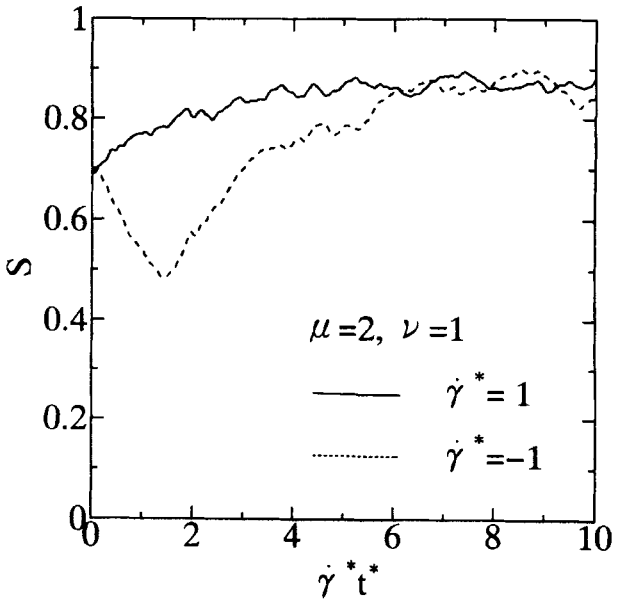

(b)

FIGURE 3 Transient behavior of orientation at the inception of shearing: (a) orientation angle; (b) order parameter. $T^* = 0.7$.

and then increases from the minimum to the same steady value as for $\dot{\gamma}^* = 1$. However, if $\dot{\gamma}^* \leqslant 0.1$, the drop of order parameter in the negative shear flow was hardly seen.

Figures 4(a) and 4(b) show the results for the initial state different from that of Figure 3; $T^* = 0.67$, $S_0 = 0.7120$, $\theta_{x0} = 36.6°$. For $\dot{\gamma}_* = -1$, the director tumbles only once in the same direction of vorticity in the initial stage of the shearing. Following the tumbling, there is a sharp reduction in the order parameter, and the order parameter becomes minimum when the director is perpendicular to the flow direction. Larson [16] predicted the decrease of the order parameter due to the tumbling for liquid crystalline polymers (LCPs) using the Doi theory [17].

3.2. Alignment and Rheological Properties

The continuum theory of Leslie-Ericksen [18–20] has been well applied to the flow of small-molecule nematics. It predicts that the orientation angle θ_x keeps a constant value regardless of shear rate in the steady shear flow for aligning nematics. However the LE theory is restricted to small rates of deformation. On the other hand, the molecular theory of Doi [17] with decoupling approximation predicts that θ_x decreases with increasing shear rate at higher shear rates while the order parameter increases [21].

Figures 5 and 6 show the shear rate dependence of orientation angle in the present simulation. It is found that the orientation angle is independent of shear rate and the value for the weak potential is smaller than that for the strong potential. Dlugogorski *et al.* [14] found that the system consisting of spheroids that interact via Gay-Berne potential built the microstructure preferentially oriented along the vorticity axis. However, we could not observe the tendency, and the director was in the shear plane even when it tilted toward the vorticity axis in the equilibrium state. Dlugogorski *et al.* [14] assumed $\sigma_e/\sigma_s = 1.9$ in the Gay-Berne potential, which means less anisotropic molecule than that used in the present calculations. Furthermore their equilibrium state as the initial condition was an isotropic phase. These differences of conditions may be the cause for discrepancy between both results.

The corresponding results for the order parameter are shown in Figures 7 and 8. The order parameter significantly increases with increasing shear rate. At high shear rates the system indicates a high orientation ($S \simeq 0.9$). Its value corresponds to that for the smectic phase in the equilibrium state; nevertheless we could not find the shear induced smectic-like phase such as Dlugogorski *et al.* [14] obtained.

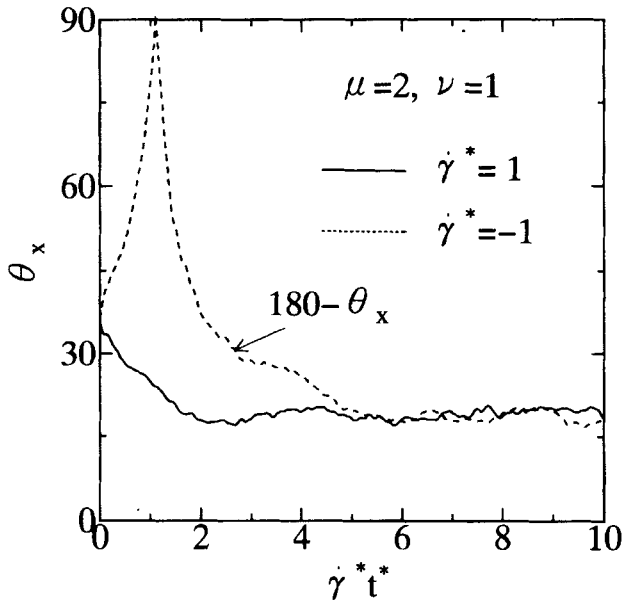

(a)

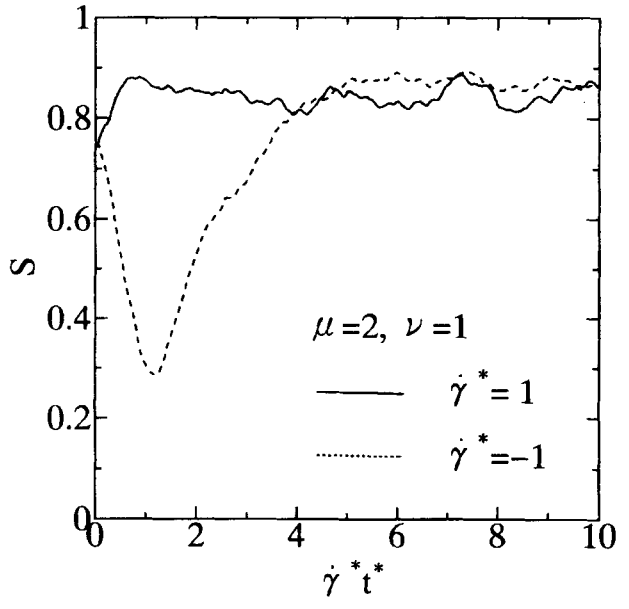

(b)

FIGURE 4 Transient behavior of orientation at the inception of shearing: (a) orientation angle; (b) order parameter. $T^* = 0.67$.

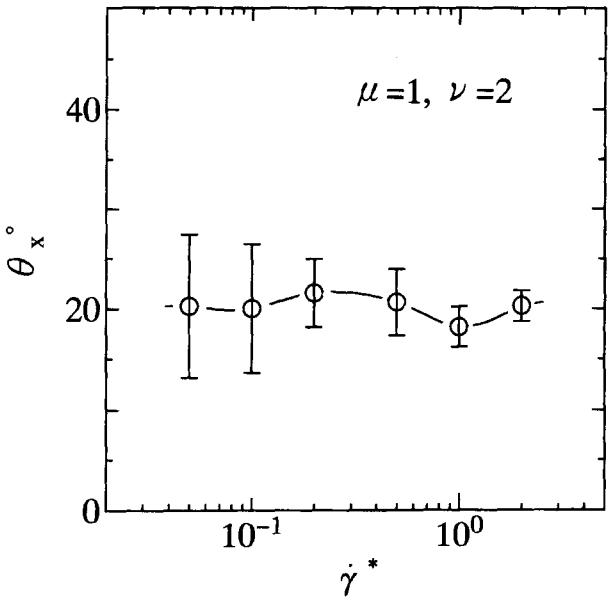

FIGURE 5 Shear rate dependence of orientation angle for the strong potential.

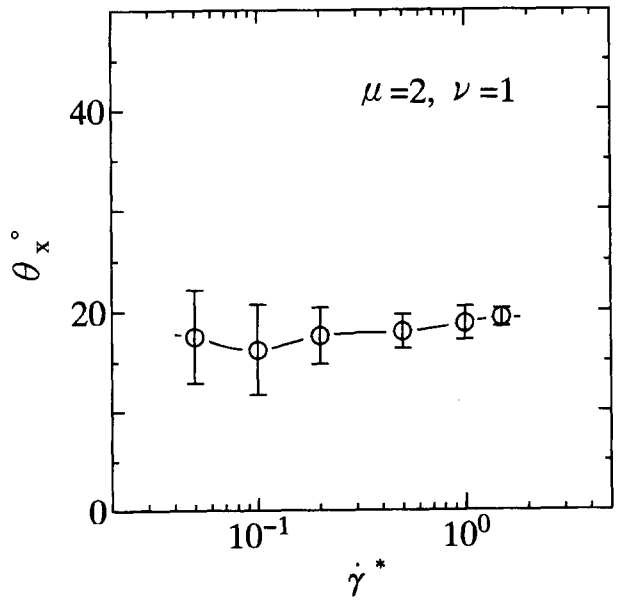

FIGURE 6 Shear rate dependence of orientation angle for the weak potential.

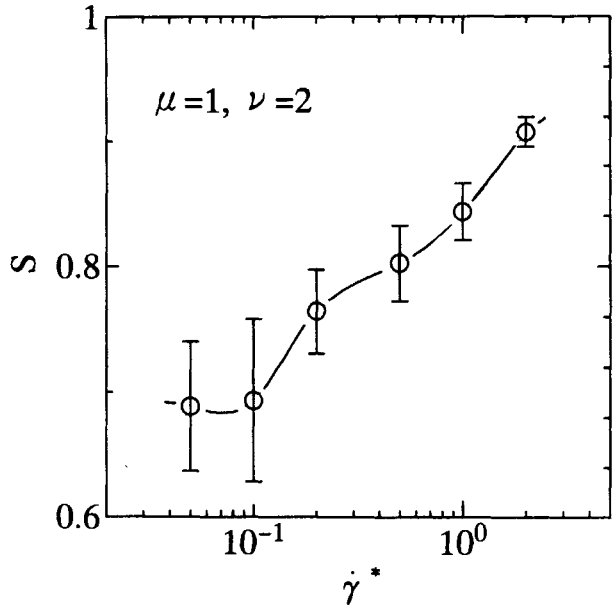

FIGURE 7 Shear rate dependence of order parameter for the strong potential.

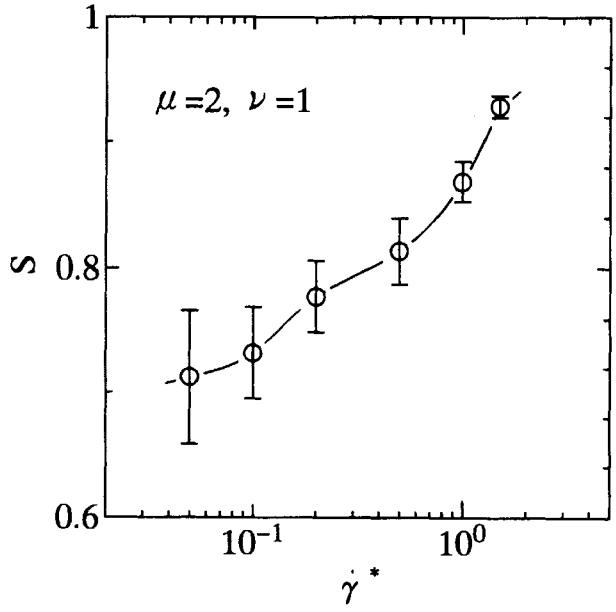

FIGURE 8 Shear rate dependence of order parameter for the weak potential.

The shear-thinning property in viscosity is found for both results at $\mu = 1$ and $\nu = 2$ (Fig. 9) and at $\mu = 2$ and $\nu = 1$ (Fig. 10). The viscosity for the weak potential shows more shear-thinning and at high shear rates its value becomes less than that for the strong potential. This is considered to be related to the fact that the order parameter for the weak potential is higher than that for the strong one.

Figure 11 shows the mean values of the first and second normal stress differences. Both N_1 and N_2 are not zero, and the sign of N_1 and N_2 are the same as for isotropic viscoelastic fluids, that is $N_1 > 0$ and $N_2 < 0$. Since the error bar for $\dot{\gamma} < 0.1$ was too large to make the results meaningful, we omitted these results from Figure 11. The ratio $|N_2/N_1|$ varies between 0.5 and 0.8. These values seem to be higher than those predicted by the Doi theory ($1/7 < N_2/N_1 < 1/5$) and for MBBA ($N_2/N_1 = 0.37$) [22], which is one of the typical small-molecule liquid crystals. However, both N_1 and N_2 are proportional to $\dot{\gamma}$ as the Leslie-Ericksen theory predicts.

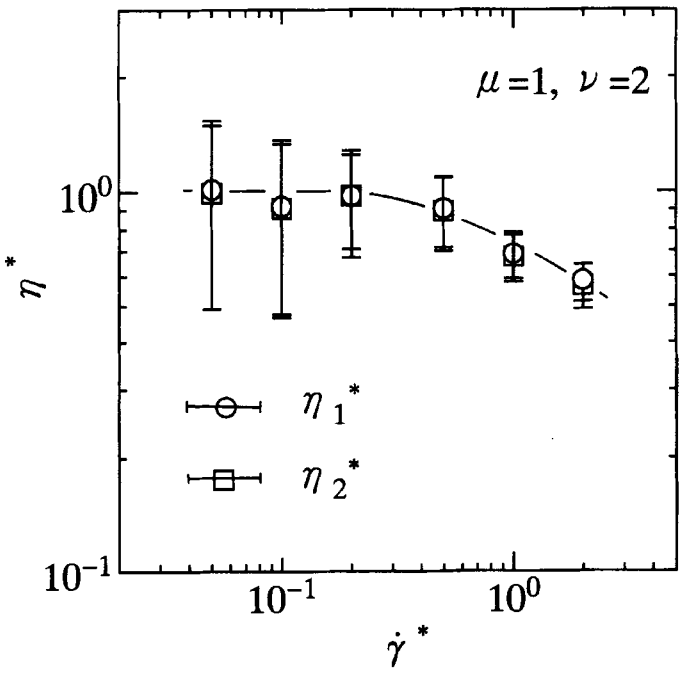

FIGURE 9 Viscosity for the strong potential.

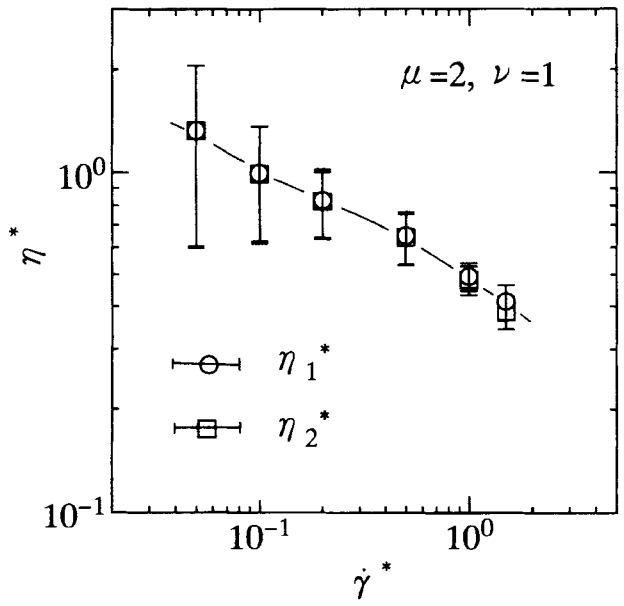

FIGURE 10 Viscosity for the weak potential.

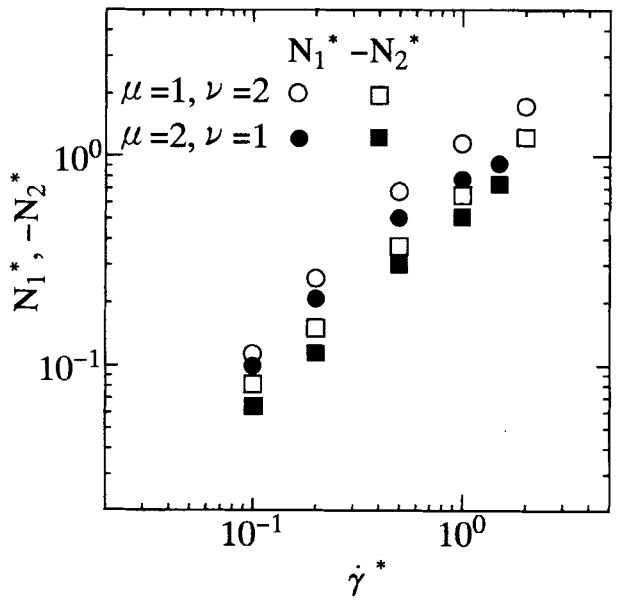

FIGURE 11 The first and second normal differences.

4. CONCLUSIONS

This work presented NEMD simulation for the shear flows of nematic liquid crystals. The SLLOD-type algorithm, which is a extension of the particle dynamics to the rigid body dynamics, well simulated the transient behavior after imposition of the shear flow on the equilibrium state; for example, the significant decrease of order parameter due to the tumbling of director. In the steady state of the shear flow, the director is inclined to the flow direction at a constant angle regardless of shear rate. The order parameter of the system, however, increases with increasing shear rate. In our studies all molecular liquids exhibit shear-thinning in viscosity and non-zero normal stress differences. Shear-induced smectic-like phase reported by Dlugogorski *et al.* [14] could not be observed and the phase obtained in our simulation was only the nematic phase. Thus we think that it is possible to simulate various behaviors such as the tumbling and wagging seen in the shear flows of real LCs and LCPs by using various of parameters in the Gay-Berne potential, density and temperature.

References

[1] J. G. Gay and B. J. Berne, *J. Chem. Phys.*, **74**, 3316 (1981).
[2] G. R. Luckhurst, R. A. Stephens and R. W. Phippen, *Liq. Crystals*, **8**, 451 (1990).
[3] E. Miguel, L. F. Rull, M. K. Chalam and K. E. Gubbins, *Molec. Phys.*, **74**, 405 (1991).
[4] R. Lukac and F. J. Vesely, *Mol. Cryst. Liq. Cryst.*, **262**, 533 (1995).
[5] M. Yoshida and H. Toriumi, *Mol. Cryst. Liq. Cryst.*, **262**, 533 (1995).
[6] S. J. Picken, W. F. van Guusteren, P. TH. van Duijnen and W. H. De Jeu, *Liq. Crystals*, **6**, 357 (1989).
[7] A. V. Komolkin, A. Laaksonen and A. Maliniak, *J. Chem. Phys.*, **101**, 4103 (1994).
[8] C. W. Cross and B. M. Fung, *J. Chem. Phys.*, **101**, 6839 (1994).
[9] D. J. Evans and G. P. Morriss, *Phys. Rev.*, **A30**, 1528 (1984).
[10] R. Edberg, G. P. Morriss and D. J. Evans, *J. Chem. Phys.*, **86**, 4555 (1986).
[11] G. P. Morriss, P. J. Davis and D. J. Evans, *J. Chem. Phys.*, **94**, 7420 (1991).
[12] P. Padilla and S. Toxvaerd, *J. Chem. Phys.*, **97**, 7687 (1992).
[13] B. Z. Dlugogorski, M. Grmela and P. J. Carreau, *J. Non-Newtonian Fluid Mech.*, **48**, 303 (1993).
[14] B. Z. Dlugogorski, M. Grmela, P. J. Carreau and G. Lebon, *J. Non-Newtonian Fluid Mech.*, **53**, 25 (1994).
[15] A. W. Lees and S. F. Edwards, *J. Phys. C: Solid State Phys.*, **5**, 1921 (1972).
[16] R. G. Larson, *Macromolecules*, **23**, 3983 (1990).
[17] M. Doi, *J. Polym. Sci.: Polym. Phys. Ed.*, **19**, 229 (1981).
[18] J. L. Ericksen, *Archs Ration. Mech. Anal.*, **4**, 231 (1960).
[19] F. M. Leslie, *Quart. J. Appl. Math.*, **19**, 357 (1966).
[20] F. M. Leslie, *Arch. Rat. Mech. Anal.*, **28**, 265 (1968).
[21] B. J. Edwards and A. N. Beris, *J. Non-Newtonian Fluid Mech.*, **35**, 51 (1990).
[22] R. G. Larson, *Constitutive Equations for Polymer Melts and Solutions*(Butterworths, **Boston**, 1988), Chap. 10, pp. 338–339.